How to cite: *Angew. Chem. Int. Ed.* **2023,** *62,* e202301489
doi.org/10.1002/anie.202301489

Bioimaging

Mixed Conductive, Injectable, and Fluorescent Supramolecular Eutectogel Composites

Miryam Criado-Gonzalez, Nuria Alegret, Alejandro M. Fracaroli, Daniele Mantione, Gregorio Guzmán-González, Rafael Del Olmo, Kentaro Tashiro, Liliana C. Tomé, Matias L. Picchio,* and David Mecerreyes**

Abstract: Eutectogels are an emerging family of soft ionic materials alternative to ionic liquid gels and organogels, offering fresh perspectives for designing functional dynamic platforms in water-free environments. Herein, the first example of mixed ionic and electronic conducting supramolecular eutectogel composites is reported. A fluorescent glutamic acid-derived low-molecular-weight gelator (LMWG) was found to self-assemble into nanofibrillar networks in deep eutectic solvents (DES)/poly(3,4-ethylenedioxythiophene) (PEDOT): chondroitin sulfate dispersions. These dynamic materials displayed excellent injectability and self-healing properties, high ionic conductivity (up to 10^{-2} S cm^{-1}), good biocompatibility, and fluorescence imaging ability. This set of features turns the mixed conducting supramolecular eutectogels into promising adaptive materials for bioimaging and electrostimulation applications.

Deep eutectic solvents (DES) are an emerging class of compounds featured by an abnormal depression of their eutectic point temperature compared to an ideal liquid mixture.[1] This negative deviation from the ideality is often associated with strong hydrogen bonding interactions between the mixture components, commonly defined as hydrogen bond acceptor (HBA) and hydrogen bond donor (HBD).[2] Since their discovery in 2003 by Abbott and coworkers,[3] DES have received increased attention as they are favorable alternatives to replace ionic liquids (ILs) and are actively being explored for a myriad of applications.[4] Similar to ILs, many DES show low vapor pressure, high ionic conductivity, and broad liquid range, but they benefit from easier preparation, low cost, non-toxicity, and biodegradability.[5] The immobilization of these intriguing solvents within polymer scaffolds leads to an innovative family of soft ionic materials called eutectogels that have very recently stepped into the spotlight.[6]

Eutectogels are commonly designed from cross-linked[7] or entangled[8] polymers, but can also be prepared from low-molecular-weight gelators (LMWGs), resulting in self-assembled networks driven by supramolecular interactions. In 2019, Smith et al. pioneered the development of supramolecular eutectogels discovering that 1,3:2,4-dibenzylidene-d-sorbitol (DBS), a low-cost commercial LMWG, could self-assemble in a DES based on choline chloride (ChCl) and alcohols/urea.[9] Only few examples of supramolecular eutectogels have recently followed up this landmark work, exploring various LMWGs such as

[*] Dr. M. Criado-Gonzalez, Dr. D. Mantione, Dr. G. Guzmán-González, Dr. R. Del Olmo, Dr. M. L. Picchio, Prof. D. Mecerreyes
POLYMAT University of the Basque Country UPV/EHU,
Joxe Mari Korta Center, Avda. Tolosa 72, 20018 Donostia-San Sebastián (Spain)
E-mail: miryam.criado@ehu.eus
mlpicchio@santafe-conicet.gov.ar
david.mecerreyes@ehu.es

Dr. N. Alegret
Center for Cooperative Research in Biomaterials (CIC biomaGUNE), Basque Research and Technology Alliance (BRTA)
Paseo de Miramón 194, 20014 Donostia-San Sebastián (Spain)

Dr. A. M. Fracaroli
Instituto de Investigaciones en Físicoquímica de Córdoba, INFIQC-CONICET, Facultad de Ciencias Químicas, Universidad Nacional de Córdoba
Ciudad Universitaria, X5000HUA Córdoba (Argentina)

Dr. D. Mantione, Dr. K. Tashiro
International Center for Materials Nanoarchitectonics (WPI-MANA), National Institute for Materials Science
1-1 Namiki, 305-0044 Tsukuba (Japan)

Dr. L. C. Tomé
LAQV-REQUIMTE, Department Of Chemistry, NOVA School Of Science And Technology, FCT NOVA, Universidade NOVA de Lisboa
2829-516 Caparica (Portugal)

Dr. M. L. Picchio
Instituto de Desarrollo Tecnológico para la Industria Química (INTEC), CONICET
Güemes 3450, 3000 Santa Fe (Argentina)

Prof. D. Mecerreyes
Ikerbasque, Basque Foundation for Science
48013 Bilbao (Spain)

guanosine,[10] halogenated DBS,[11] d-gluconic acetal,[12] and bisgluconamide derivatives.[13] Surprisingly, although scientific efforts have been devoted to developing purely ionic-conducting systems, mixed ionic-electronic conducting supramolecular eutectogel composites have not been considered until now. In this vein, organic mixed ionic-electronic conductors (OMIECs), like poly(3,4-ethylenedioxythiophene) (PEDOT) with enhanced charge storage and coupled transport properties could expand the applicability of these deep eutectic soft ionic materials.[14] For instance, OMIECs open the gate to electrostimulation or biosensing, and consequently, mixed conducting supramolecular eutectogels could find new routes in tissue regeneration, accelerated wound healing, and iontophoretic ocular drug delivery, among others.[15]

Since hydrogen-bonding interactions are inherently present in most DES, the supramolecular assembly of classical LMWGs is not always given. Herein a new phenanthroline-modified glutamic acid derivative was identified as a eutectogelator in the presence of different choline chloride (ChCl)-based DES and combined with PEDOT:Chondroitin sulfate (ChS). These specific DES were chosen as they have been shown to be biocompatible and non-cytotoxic,[16] and have a strong dissolution power for hydrophobic drugs.[17] In this regard, with a view toward biomedical applications, we decided to use ChS polysaccharide for PEDOT stabilization as it has proven to promote chondrogenic differentiation and re-epithelialization.[18] Moreover, to the best of our knowledge, there are no comparative studies between supramolecular eutectogels and their ionic liquid gels or iongels counterparts. Thus, we also provide helpful insights into this matter by comparing ChCl-based DES with cholinium-derived ILs.

Firstly, the ability of new phenanthroline-modified glutamic acid LMWG (Figure S1) to jellify DES was investigated. The supramolecular eutectogels were formed by hot dissolution of the LMWG in the DES, followed by a cooling step at room temperature to trigger the gelation process (Scheme 1a). Different DES, based on ChCl and three HBDs, namely glycerol (Gly=G), lactic acid (LacAc=L), and glycolic acid (GlyAc=GA), were tested (Figure 1a). Inverted vial tests show the eutectogel formation in the case of $eGel_G$ and $eGel_{GA}$, but not for $eGel_L$. The use of acidic DES resulted in orange gels, probably because of the phenanthroline group protonation. The FTIR spectrum of the LMGW shows characteristic peaks at 1721, 1694, 1660 (C=O ν of *Boc*, *Fmoc*, and glutamic acid residue), 1553 (ring skeleton), 1157 (C–H δ ip), and 739 cm^{-1} (C=C δ) (Figure S2). After gel formation, the main peaks of the LMWG are evidenced without significant signal shifts. However, the relative intensity of the C–H δ ip and C=C δ peaks changed in the eutectogel, suggesting that π–π interactions play an essential role in gel formation. The structural organization of the eutectogel $eGel_G3$ was further investigated by circular dichroism (CD) (Figure S3). The CD spectrum of $eGel_G3$ shows a positive band at 196 nm and a strong negative band at 221 nm, which is the signature of β-sheet structures.[19] Besides, the maxima at 251 nm is characteristic of stacking interaction of the aromatic units of

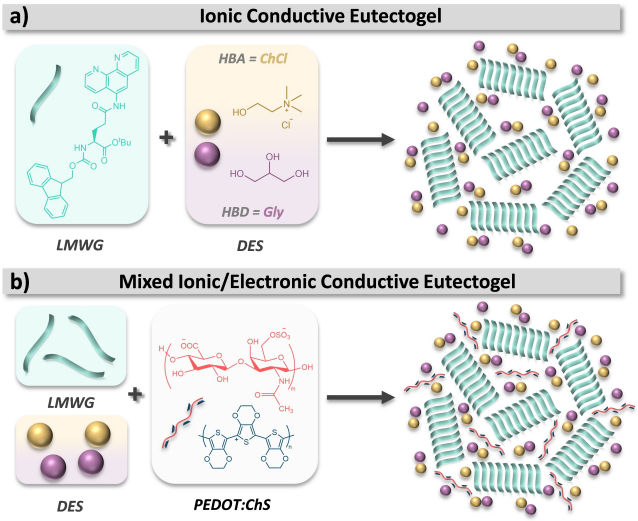

Scheme 1. (a) Single ionic conductive eutectogel formed by the supramolecular interaction of a glutamic acid-derived LMWG and a DES. (b) Hybrid mixed ionic/electronic conductive eutectogel composite formed by the supramolecular interaction of LMWG, DES, and PEDOT:ChS.

the LMWG, and the negative bands at 271 and 308 nm are attributed to the offset face-to-face stacking of the Fmoc moieties and the fluorenyl absorption, respectively.[20] The viscoelastic properties of the eutectogels, particularly the elastic modulus (G′) and loss modulus (G″), were measured by dynamic oscillatory rheology. Strain sweeps allow us to determine the linear viscoelastic regime (LVR) up to 3 % strain and the total gel to sol transition (G″ > G′) from 40 % strain. At 1 % strain, in the LVR zone, G′ ($\approx 10^4$ Pa) is higher than G″ ($\approx 10^3$ Pa), which is the condition of the gel state and keeps stable in the whole frequency range (Figure S4). Injectable and self-healable gels are actively searched for minimally invasive treatments in biomedicine.[21] Thus, these properties were studied by dynamic step strain tests (Figure 1b). At low strains (γ = 1 %), G′ is higher than G″ for both formed eutectogels, $eGel_G3$ (G′ = 350 Pa > G″ = 90 Pa), and $eGel_{GA}3$ (G′ = 1500 Pa > G″ = 180 Pa), proving the gel state before injection. Then, the samples were subjected to high strains (γ = 1000 %) during short times (180 s), mimicking the pass of the gel through the needle, taking place a gel to sol transition (G″ > G′). Subsequently, by ceasing to apply great efforts and applying low strains (γ = 1 %) again, this behavior was reversed in the case of $eGel_G3$ eutectogels (G′ = 120 Pa > G″ = 40 Pa), proving the recovery of the gel state after injection, whereas $eGel_{GA}3$ eutectogels barely recovered the gel state (G′ = 40 Pa ≈ G″ = 25 Pa), exhibiting modulus far from the initial values. These results show that only the $eGel_G3$ eutectogels possessed self-healing and injectability properties, and thus, the $eGel_G3$ were selected for further experiments. Note that similar elastic moduli have been found for xantham gum eutectogels formed in Gly/ChCl DES.[22]

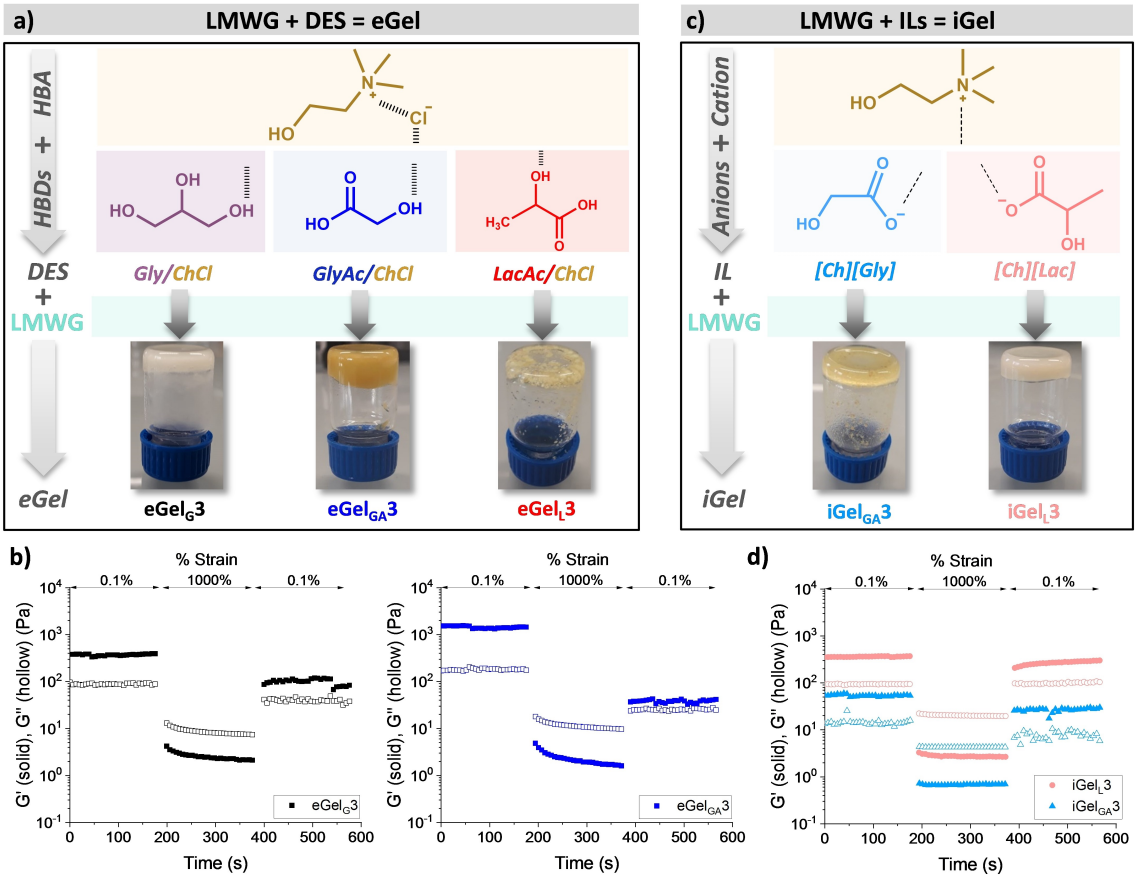

Figure 1. (a) Eutectogels formed by the supramolecular interactions of different choline chloride based DES with a glutamic acid-derived LMWG, with their corresponding inverted vial test pictures. [LMWG] = 3 % w/v. (b) Dynamic step-strain amplitude tests of the eutectogels, $eGel_G3$ and $eGel_{GA}3$. (c) Iongels formed by the supramolecular interactions of cholinium-based ionic liquids and the LMWG, with their corresponding inverted vial test pictures. [LMWG] = 3 % w/v. (d) Dynamic step-strain amplitude tests of the iongels, $iGel_L3$ and $iGel_{GA}3$.

Once the ability of the glutamic acid-derived gelator to form supramolecular networks in DES was confirmed, the comparison of eutectogels *vs.* iongels was addressed. The iongels were prepared by the hot dissolution of the LMWG in cholinium lactate (ChLac) and cholinium glycolate (ChGly) ILs (Figure S5–S6) and subsequent cooling (Figure 1c). The rheological tests show that both the iongels have self-healing properties with the recovery of the gel state after the low-high-low strain cycle, $iGel_{GA}3$ ($G' = 60$ Pa $> G'' = 30$ Pa), and $iGel_L3$ ($G' = 360$ Pa $> G'' = 300$ Pa) (Figure 1d). Moreover, we found that using DES gave gels with enhanced mechanical properties, showing higher G' values than the gel materials prepared with ILs (Figure S7). Besides, the ionic conductivity (σ_i) was determined by electrochemical impedance spectroscopy from 23 to 85 °C (Figure 2a). The $eGel_G3$ eutectogels have higher ionic conductivity ($\sigma_i = 10^{-2}$ S cm^{-1}) than that of $iGel_L3$ iongels ($\sigma_i = 10^{-3}$ S cm^{-1}), with a typical linear dependence of σ_i with the temperature as a consequence of the favored carrier mobility. The higher ionic conductivity of $eGel_G3$ is probably due to the significatively lower viscosity of Gly/ChCl DES compared with [Ch][Lac] ionic liquid, favoring the ionic mobility. These σ_i values are in agreement with previous works related to eutectogels formed by a glycerol-based DES with polymers, i.e., gelatin, polyacrylic acid (PAA),[8a,23] or other LMWGs such as DBS.[9]

Considering the superior mechanical and ionic conductive properties of the prepared eutectogels, the $eGel_G$ was further studied in detail. The eutectogel exhibited a fibrillary morphology with fiber diameters lower than 50 nm, as observed by transmission electron microscopy (TEM) (Figure 2b). The influence of the LMWG concentration on the eutectogel mechanical properties was analyzed by rheology. Figure 2c shows an increase of G' with the LMWG concentration, from 350 Pa for 3 % LMWG to 2150 Pa for 5 % LMWG. The yield strain is not significantly affected by the LMWG concentration showing a gel-to-sol transition from 20 % strain in all cases (Figure S8). Nevertheless, the self-healing properties are adversely affected (Figure 2d) with lower G' recovery with respect to the initial G' values as the LMWG concentration increases.

The mixed ionic/electronic supramolecular eutectogel composites were prepared by adding a conducting polymer PEDOT:ChS to the selected LMWG + DES mixture during the heating step, to be then cooled down until room temperature to trigger the gelation process (Scheme 1b).

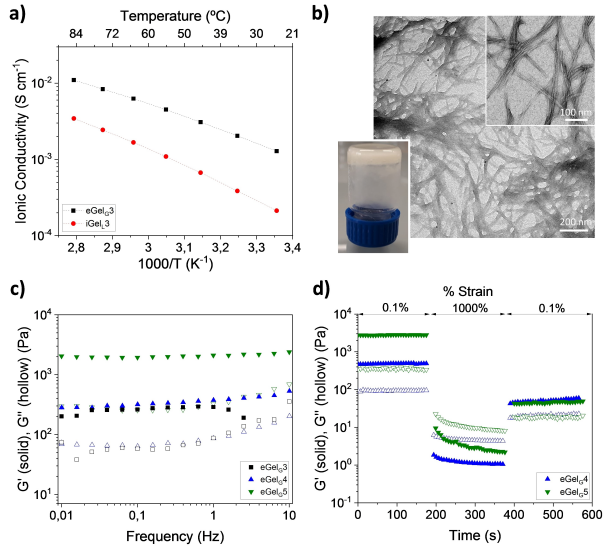

Figure 2. (a) Ionic conductivity of the eutectogel $eGel_G3$ and the iongel $iGel_L3$ at different temperatures. (b) TEM image of the eutectogel $eGel_G3$. The inset shows the eutectogel' visual appearance. (c) Storage modulus (G′) and loss modulus (G″) as a function of the frequency of the eutectogels $eGel_G3$, $eGel_G4$ and $eGel_G5$. (d) Dynamic step-strain amplitude tests of $eGel_G4$ and $eGel_G5$ eutectogels.

The presence of PEDOT:ChS did not affect the gelation kinetic as determined by the inverted tube tests, which show the eutectogel composite formation in the presence of PEDOT:ChS, and whose morphology was further visualized by TEM (Figure 3a). In that case, apart from the characteristic fibers of the LMWG self-assembly in the DES, PEDOT:ChS aggregates are also distinguished and homogeneously distributed along the whole eutectogel composite network. As controls (Figure S9), the TEM picture of the DES solution does not show any structural conformation, while the PEDOT:ChS dispersion presents the same morphology as aggregates observed in Figure 3a and Figure S10, confirming the successful incorporation of the electronic component PEDOT:ChS in the eutectogel. FTIR spectrum of PEDOT:ChS display typical peaks at 1515 (skeletal vibrations), 1314 ($RO–SO_3^-$ ν as), 1185 ($RO–SO_3^-$ ν sy), 1048 (C–O–C ν as), 974 (C–H δ oop), and 825 cm^{-1} (S–O ν) (Figure S2). However, these vibrational modes were hard to identify in $eGel_G3$/CP as they overlap with the intense peaks of the DES. An increase of the PEDOT:ChS concentration in the eutectogel composites, from 2 to 5 % w/v, produces an increase of the elastic modulus, from 1300 to 7400 Pa for $eGel_G3$, and from 2100 to 4000 Pa for $eGel_G4$ (Figure 3b and Figure S11). Concerning the influence of PEDOT:ChS concentration on the self-healing properties, $eGel_G3$/CP2 eutectogel composites present better G′ recovery values than $eGel_G3$/CP5 (Figure 3c and Figure S12), possibly because of higher concentration of PEDOT:ChS aggregates impact the crosslinking density of the supramolecular network, making the resulting materials more brittle. This effect has also been found in blends of PEDOT:PSS (polystyrene sulfonate, PSS) with waterborne polyurethane (WPU),[24] and with a vinyl resin containing poly(ethylene glycol) diacrylate (PEGDA),[25] which both types of materials exhibited a considerable reduction of the elongation at break with the PEDOT:PSS loading. The effect of the temperature on the viscoelastic properties was also studied (Figure S13), and the results demonstrate that there is not any impact on G′ values when the temperature changes from room temperature (20 °C) to extreme body temperature conditions (42 °C). Importantly, the presence of PEDOT:ChS affords electronic conductivity (σ_e) to the eutectogel composites that increases with the PEDOT:ChS loading, as measured by direct current (DC) polarization (Figure S14). The control eutectogel $eGel_G3$ without PEDOT delivered a negligible current, whereas composite eutectogels $eGel_G3$/CP2 and $eGel_G3$/CP5 reached currents of 0.06 mA and 0.82 mA, respectively, after 1 h. Considering the Ohm's law and the geometric parameters, these values were translated in electronic conductivity: $\sigma_e = 0$ for $eGel_G3$, $\sigma_e = 1.6 \cdot 10^{-5}$ S cm^{-1} for $eGel_G3$/CP2, and $\sigma_e = 2.1 \cdot 10^{-4}$ S cm^{-1} for $eGel_G3$/CP5. This effect can be explained by the fact that $eGel_G3$/CP5 possesses a higher percolation path which gives rise to an efficient hopping between π–π stacked chains and higher electronic conductivity than $eGel_G3$/CP2 that could achieve a percolation threshold decreasing the electronic conductivity.[26] On the other hand, the ionic conductivity (Figure 3d) remains unaffected ($\sigma_i = 10^{-2}$ S cm^{-1}), and mixed ionic/electronic eutectogel composites present the typical σ_i linear dependence with the temperature as in the case of simple ion conductive eutectogels. Note that although PEDOT is a mixed conductor, a negligible contribution to the overall ionic conductivity is observed, probably because

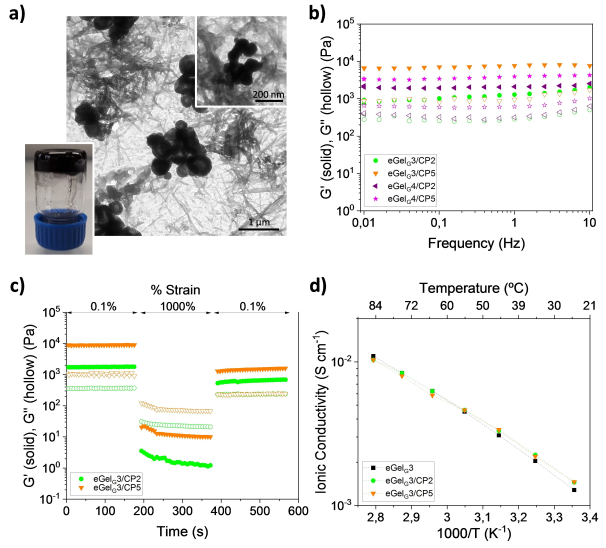

Figure 3. (a) TEM image of the eutectogel composite $eGel_G3$/CP2. The inset shows the eutectogel' visual appearance. (b) Storage modulus (G′) and loss modulus (G″) as a function of the frequency of the mixed ionic/conductive eutectogel composites $eGel_G3$/CP2, $eGel_G3$/CP5, $eGel_G4$/CP2 and $eGel_G4$/CP5. (c) Dynamic step-strain amplitude tests, and (d) Ionic conductivity at different temperatures of the eutectogel composites, $eGel_G3$/CP2 and $eGel_G3$/CP5.

of its low concentration in the eutectogel composite compared with the eutectic carrier.

Interestingly, the Fmoc and phenanthroline groups in the LMGW endow the eutectogels with intrinsic fluorescence, which is very useful for bioimaging (Figure 4a). Both kinds of eutectogels, single ionic conductive and mixed ionic/electronic conductive gels, display similar fluorescence spectra with maximum emission peaks in the blue region at 408 and 435 nm, meaning that the LMWG fluorescence is not affected by the incorporation of PEDOT:ChS within the eutectogel network. Previously to study biocompatibility, the eutectogels' stability in physiological mimicking conditions (Phosphate buffered saline (PBS) at pH 7.4 and 37 °C) was tested (Figure S15). In the case of single ionic conductive eutectogels ($eGel_G3$), a partial disaggregation of the gel structure is observed after 48 h, while the mixed ionic/electronic conductive eutectogel composites ($eGel_G3/CP2$) remains stable, at least, up to 72 h. The supramolecular H-bonding interactions between the LMWG and the DES can be broken in presence of an ionic media such as PBS, which can interact electrostatically with the DES leading to a partial disassembly of the eutectogel. This effect is prevented when PEDOT:ChS is incorporated within the eutectogel network due to the electrostatic interactions of the long chains of the polymer ChS with the LMWG, which stabilize the eutectogel network becoming it more resistant and preventing its disintegration in presence of PBS. In vitro cell tests were performed by placing the eutectogels in contact with iPSC cells. Regarding the cytotoxicity tests (Figure 4b), the results show no significant differences in the absorbance for the eutectogels when compared to the Matrigel-coated well-plate used as a control (CTL). This means that the cell survival is not altered in contact with the eutectogels, demonstrating that they are non-cytotoxic. Besides, Figure 4c shows a slight increase in cell viability in the mixed ionic/electronic conductive eutectogel composites, $eGel_G3/CP$, compared to that of the single ionic conductive eutectogel, $eGel_G3$ (without PEDOT:ChS in the network). This behavior can be attributed to the fact that conductive materials can promote proliferation and differentiation when responsive cells are cultured on top or within them.[27] In fact, the results obtained by direct current (DC) polarization tests showed that both $eGel_G3/CP2$ and $eGel_G3/CP5$ eutectogel composites display additional electronic conductivity when compared to the $eGel_G3$, which only presents ionic conductivity. Therefore, mixed ionic/electronic eutectogel composites, $eGel_G3/CP2$, and $eGel_G3/CP5$, may provide an extra electrical stimulation *per se* to the cells in contact with them, favoring the chemical exchanges and signal communications among the cells at the cell membrane-material interface, inducing their proliferation.[28] This preliminary growth tendency is a first finding for mixed ionic/electronic eutectogel composite systems that needs to be explored in detail, and further experiments involving different cellular models and external electrical stimuli will be conducted in the future.

Finally, the proof of concept of the developed $eGel_G3/CP2$ eutectogel composites to be employed as an agent for local and minimally invasive bioimaging applications was assessed with mice bodies, which were not explicitly sacrificed for this experiment. The eutectogel composite was injected subcutaneously in a local part of the mouse's ear (Figure 4d). Then, the mouse's ear was irradiated, observing clearly the fluorescence light emitted at the local part of the tissue where the eutectogel composite had been previously injected (Figure 4e). The employment of the eutectogel in other body areas, such as rodent tails, was also tested

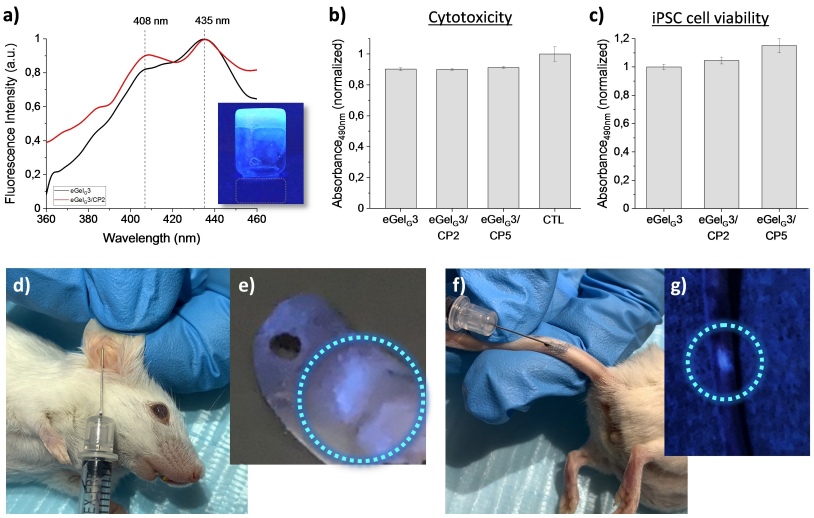

Figure 4. (a) Fluorescence spectra of the eutectogels $eGel_G3$ and $eGel_G3/CP2$. The inset shows a picture of the fluorescent eutectogel $eGel_G3$ when it is irradiated with a UV lamp at 354 nm. LDH assays to determine the (b) cytotoxicity and (c) cell viability of the eutectogels in contact with iPSC cells (mean and standard deviation from $n=4$). In vivo injectability of the eutectogel composites in mice at different areas: (d) ears and (e) the localized bioimaging fluorescence showed by the dashed blue circle, (f) tails and (g) the localized bioimaging fluorescence showed by the dashed blue circle. UV excitation at 254 nm.

(Figure 4f–g and Videos S1–S2), corroborating the localized bioimaging properties in different body tissues.

In summary, mixed ionic/electronic conductive eutectogel composites were successfully formed by combining a fluorescent glutamic acid-derived LMWG with PEDOT:ChS and ChCl-based DES. Among different DES tested, supramolecular eutectogels formed with Gly/ChCl DES showed the best self-healing and injectability properties. The comparison between the ChCl-based eutectogels (eGel) and cholinium-based iongels (iGel) was also tackled, revealing the enhanced ionic conductivity properties of the eutectogels ($\approx 10^{-2}$ S cm^{-2}) compared to iongels ($\approx 10^{-3}$ S cm^{-3}). The biological tests confirmed the non-cytotoxic properties of the eutectogels in contact with iPSC cells. Furthermore, the eutectogel composites were successfully injected in subcutaneous local areas of rats exhibiting a localized fluorescence, which opens the way to potential minimally invasive bioimaging applications.

Acknowledgements

This work was supported by Marie Sklodowska-Curie Research and Innovation Staff Exchanges (RISE) under the grant agreement No 823989 "IONBIKE". The financial support received from CONICET and ANPCyT (Argentina) is also gratefully acknowledged. M. C.-G. thanks Emakiker Grant Program of POLYMAT. L. C. T. is grateful to Fundação para a Ciência e a Tecnologia (FCT/MCTES) in Portugal for her research contract under Scientific Employment Stimulus (2020.01555.CEECIND), and Associate Laboratory for Green Chemistry—LAQV, which is also financed by FCT/MCTES (UIDB/50006/2020 and UIDP/50006/2020). D. M. thanks "Ayuda RYC2021-031668-I financiada por MCIN/AEI/10.13039/501100011033 y por la Unión Europea NextGenerationEU/PRTR". The authors thank the technical and human support provided by SGIker (UPV/EHU/ERDF, EU).

Conflict of Interest

The authors declare no conflict of interest.

Data Availability Statement

The data that support the findings of this study are available from the corresponding author upon reasonable request.

Keywords: Bioimaging · Deep Eutectic Solvents · Ionic Liquids · Organic Mixed Ionic–Electronic Conductors · Supramolecular Eutectogels

[1] M. A. R. Martins, S. P. Pinho, J. A. P. Coutinho, *J. Solution Chem.* **2019**, *48*, 962–982.
[2] a) D. Yu, Z. Xue, T. Mu, *Chem. Soc. Rev.* **2021**, *50*, 8596–8638; b) E. L. Smith, A. P. Abbott, K. S. Ryder, *Chem. Rev.* **2014**, *114*, 11060–11082.
[3] A. P. Abbott, G. Capper, D. L. Davies, R. K. Rasheed, V. Tambyrajah, *Chem. Commun.* **2003**, 70–71.
[4] a) F. M. Perna, P. Vitale, V. Capriati, *Curr. Opin. Green Sustainable Chem.* **2020**, *21*, 27–33; b) M. L. Picchio, D. Minudri, D. Mantione, M. Criado-Gonzalez, G. Guzmán-González, R. Schmarsow, A. J. Müller, L. C. Tomé, R. J. Minari, D. Mecerreyes, *ACS Sustainable Chem. Eng.* **2022**, *10*, 8135–8142.
[5] a) A. Paiva, R. Craveiro, I. Aroso, M. Martins, R. L. Reis, A. R. C. Duarte, *ACS Sustainable Chem. Eng.* **2014**, *2*, 1063–1071; b) Y. Liu, J. B. Friesen, J. B. McAlpine, D. C. Lankin, S.-N. Chen, G. F. Pauli, *J. Nat. Prod.* **2018**, *81*, 679–690.
[6] a) J. Wang, S. Zhang, Z. Ma, L. Yan, *Green Chem.* **2021**, *2*, 359–367; b) L. C. Tomé, D. Mecerreyes, *J. Phys. Chem. B* **2020**, *124*, 8465–8478.
[7] G. Li, Z. Deng, M. Cai, K. Huang, M. Guo, P. Zhang, X. Hou, Y. Zhang, Y. Wang, Y. Wang, X. Wu, C. F. Guo, *npj Flexible Electron.* **2021**, *5*, 23.
[8] a) M. L. Picchio, A. Gallastegui, N. Casado, N. Lopez-Larrea, B. Marchiori, I. del Agua, M. Criado-Gonzalez, D. Mantione, R. J. Minari, D. Mecerreyes, *Adv. Mater. Technol.* **2022**, *7*, 2101680; b) H. Zhang, N. Tang, X. Yu, M.-H. Li, J. Hu, *Adv. Funct. Mater.* **2022**, *32*, 2206305.
[9] J. Ruiz-Olles, P. Slavik, N. K. Whitelaw, D. K. Smith, *Angew. Chem. Int. Ed.* **2019**, *58*, 4173–4178.
[10] C. Gu, Y. Peng, J. Li, H. Wang, X.-Q. Xie, X. Cao, C.-S. Liu, *Angew. Chem. Int. Ed.* **2020**, *59*, 18768–18773.
[11] K. Fan, L. Wang, W. Wei, F. Wen, Y. Xu, X. Zhang, X. Guan, *Chem. Eng. J.* **2022**, *441*, 136026.
[12] a) B. Zhang, H. Sun, Y. Huang, B. Zhang, F. Wang, J. Song, *Chem. Eng. J.* **2021**, *425*, 131518; b) H. Sun, B. Zhang, L. Lu, Z. Chen, Y. Huo, W. Li, B. Zhang, J. Song, *Chem. Eng. J.* **2023**, *451*, 139051.
[13] K. Wang, H. Wang, J. Li, Y. Liang, X.-Q. Xie, J. Liu, C. Gu, Y. Zhang, G. Zhang, C.-S. Liu, *Mater. Horiz.* **2021**, *8*, 2520–2532.
[14] a) B. D. Paulsen, K. Tybrandt, E. Stavrinidou, J. Rivnay, *Nat. Mater.* **2020**, *19*, 13–26; b) D. Ohayon, S. Inal, *Adv. Mater.* **2020**, *32*, 2001439; c) M. ElMahmoudy, S. Inal, A. Charrier, I. Uguz, G. G. Malliaras, S. Sanaur, *Macromol. Mater. Eng.* **2017**, *302*, 1600497.
[15] S. Zhao, A. S. Mehta, M. Zhao, *Cell. Mol. Life Sci.* **2020**, *77*, 2681–2699.
[16] a) I. P. E. Macário, H. Oliveira, A. C. Menezes, S. P. M. Ventura, J. L. Pereira, A. M. M. Gonçalves, J. A. P. Coutinho, F. J. M. Gonçalves, *Sci. Rep.* **2019**, *9*, 3932; b) M. Petkovic, J. L. Ferguson, H. Q. N. Gunaratne, R. Ferreira, M. C. Leitão, K. R. Seddon, L. P. N. Rebelo, C. S. Pereira, *Green Chem.* **2010**, *12*, 643–649.
[17] T. Jeliński, M. Przybyłek, P. Cysewski, *Pharm. Res.* **2019**, *36*, 116.
[18] a) B. Corradetti, F. Taraballi, S. Minardi, J. Van Eps, F. Cabrera, L. W. Francis, S. A. Gazze, M. Ferrari, B. K. Weiner, E. Tasciotti, *Stem Cells Transl. Med.* **2016**, *5*, 670–682; b) M. Concha, A. Vidal, A. Giacaman, J. Ojeda, F. Pavicic, F. A. Oyarzun-Ampuero, C. Torres, M. Cabrera, I. Moreno-Villoslada, S. L. Orellana, *J. Biomed. Mater. Res. Part B* **2018**, *106*, 2464–2471.
[19] N. J. Greenfield, *Nat. Protoc.* **2006**, *1*, 2876–2890.
[20] M. Criado-Gonzalez, D. Wagner, J. Rodon Fores, C. Blanck, M. Schmutz, A. Chaumont, M. Rabineau, J. B. Schlenoff, G. Fleith, J. Combet, P. Schaaf, L. Jierry, F. Boulmedais, *Chem. Mater.* **2020**, *32*, 1946–1956.
[21] a) M. Criado-Gonzalez, E. Espinosa-Cano, L. Rojo, F. Boulmedais, M. R. Aguilar, R. Hernández, *ACS Appl. Mater.*

Interfaces **2022**, *14*, 10068–10080; b) T. Birman, D. Seliktar, *Adv. Funct. Mater.* **2021**, *31*, 2100628.
[22] C. Zeng, H. Zhao, Z. Wan, Q. Xiao, H. Xia, S. Guo, *RSC Adv.* **2020**, *10*, 28376–28382.
[23] J. Wang, Z. Ma, Y. Wang, J. Shao, L. Yan, *Macromol. Rapid Commun.* **2021**, *42*, 2000445.
[24] H. He, J. Ouyang, *Acc. Mater. Res.* **2020**, *1*, 146–157.
[25] N. Lopez-Larrea, M. Criado-Gonzalez, A. Dominguez-Alfaro, N. Alegret, I. d. Agua, B. Marchiori, D. Mecerreyes, *ACS Appl. Polym. Mater.* **2022**, *4*, 6749–6759.
[26] M. Berggren, X. Crispin, S. Fabiano, M. P. Jonsson, D. T. Simon, E. Stavrinidou, K. Tybrandt, I. Zozoulenko, *Adv. Mater.* **2019**, *31*, 1805813.
[27] a) A. G. Guex, J. L. Puetzer, A. Armgarth, E. Littmann, E. Stavrinidou, E. P. Giannelis, G. G. Malliaras, M. M. Stevens, *Acta Biomater.* **2017**, *62*, 91–101; b) S. Wang, C. Sun, S. Guan, W. Li, J. Xu, D. Ge, M. Zhuang, T. Liu, X. Ma, *J. Mater. Chem. B* **2017**, *5*, 4774–4788.
[28] A. Dominguez-Alfaro, M. Criado-Gonzalez, E. Gabirondo, H. Lasa-Fernández, J. L. Olmedo-Martínez, N. Casado, N. Alegret, A. J. Müller, H. Sardon, A. Vallejo-Illarramendi, D. Mecerreyes, *Polym. Chem.* **2022**, *13*, 109–120.

Manuscript received: January 30, 2023
Accepted manuscript online: May 2, 2023
Version of record online: May 15, 2023